SVM for Constellation Shaped 8QAM PON System

Abstract: Nonlinearity impairments and distortions have been bothering the bandwidth constrained passive optical network (PON) system for a long time and limiting the development of capacity in the PON system. Unlike other works concentrating on the exploration of the complex equalization algorithm, we investigate the potential of constellation shaping joint support vector machine (SVM) classification scheme. At the transmitter side, the 8 quadrature amplitude modulation (8QAM) constellation is shaped into three designs to mitigate the influence of noise and distortions in the PON channel. On the receiver side, simple multi-class linear SVM classifiers are utilized to replace complex equalization methods. Simulation results show that with the bandwidth of 25 GHz and overall bitrate of 50 Gbit/s, at 10 dBm input optical power of a 20 km standard single mode fiber (SSMF), and under a hard-decision forward error correction (FEC) threshold, transmission can be realized by employing Circular (4, 4) shaped 8QAM joint SVM classifier at the maximal power budget of 37.5 dB.

Keywords: passive optical networks; support vector machine; geometrically shaping; constellation classification; digital signal processing

LI Zhongya[1,3], CHEN Rui[2,3], HUANG Xingang[2], ZHANG Junwen[1,3], NIU Wenqing[1,3], LU Qiuyi[1,3], CHI Nan[1]

(1. Key Laboratory for Information Science of Electromagnetic Waves, Fudan University, Shanghai 200433, China;
2. ZTE Corporation, Shenzhen 518057, China;
3. Department of Communication Science and Engineering, School of Information Science and Technology, Fudan University, Shanghai 200433, China)

DOI: 10.12142/ZTECOM.2022S1009

http://kns.cnki.net/kcms/detail/34.1294.TN.20211122.1958.001.html, published online November 23, 2021

Manuscript received: 2021-07-25

Citation (IEEE Format): Z. Y. Li, R. Chen, X. G. Huang, et al., "SVM for constellation shaped 8QAM PON system," *ZTE Communications*, vol. 20, no. S1, pp. 64 - 71, Jan. 2022. doi: 10.12142/ZTECOM.2022S1009.

1 Introduction

The newly emerged application scenarios of access networks such as high-definition video streaming services, virtual reality and cloud computing are all driving capacity upgradation for next-generation (NG) passive optical networks (PONs), which is highly recognized for their low cost and flexible advantages. In the meantime, organizations like IEEE 802.3ca and ITU-T are working on the standardization of their 50 Gbit/s/λ^{-1} PON[1], and feasible 100 Gbit/s solutions are under investigation[2 - 3]. Low-cost intensity modulation and direct detection (IM/DD) transmission schemes have been demonstrated using 10 Gbit/s transmitters[3 - 5]. To achieve high-speed PONs with bandwidth limited optics components, advanced modulation formats and effective digital signal processing (DSP) are the central research topics[6]. Electrical/optical duo-binary[3], pulse amplitude modulation (PAM) [7], and carrierless amplitude and phase (CAP) modulation[8] have been widely investigated for a potential low-cost solution for medium- and long reach-PON systems. Related works suggest that compared with non-return zero (NRZ), PAM, or orthogonal frequency division multiplexing (OFDM), the IM/DD based CAP modulation scheme has great potential in the optical transmission system for its advantages of low power consumption, high spectrum efficiency, and low cost[9]. But limited works have been devoted to researching the applicability of CAP modulation in the PON system. In this work, we transmit single band CAP modulated 8QAM signals in the PON system and provide the performance analysis.

In fiber-optic communication systems, higher-order QAM modulation leads to higher spectral efficiency, but at the same time, inter-symbol interference (ISI) increases, which demands higher signal-to-noise ratios (SNRs) to ensure reliable system transmission. However, for legacy optics based high capacity PON systems, the bandwidth limitation and fiber dispersion would induce severe distortion to signals and lead to lower SNR. To overcome impairments, several DSP methods are introduced including feed forward equalization (FFE), decision feed-back equalization (DFE)[10], Volterra (VOT) nonlinear equalization, least-mean-square (LMS) equalization[6], and digital pre-equalization. Such schemes bring great costs on computational complexity and are impractical in real deploy-

This work was partially supported by the NSFC project (No. 61925104, No. 62031011), and by ZTE Industry-Academia-Research Cooperation Funds under Grant No. HC-CN-20191231006.

ments. In Refs. [11 – 12] support vector machines (SVMs) are used for QAM classification, which is an unusual way to mitigate signal distortions. Moreover, a geometrically shaping technology is applied to QAM signals in Ref. [12] to further improve its resistance to noise. However, the related research is carried out in a 50 m fiber and visible light system, of which channel characteristics, such as the bandwidth, dispersion, attenuation, and origins of nonlinearity, are quite different from the PON systems. The idea of separating computational pressures onto transmitter and receiver sides is novel but needs to be assessed and optimized in the cost-sensitive PON system. Thus, it is still a challenge to develop a reliable and low-cost solution to dealing with the linear and nonlinear distortions in the bandwidth limited high speed PON system.

To cope with this problem, we adopt a cheap scheme employing the constellation shaping technique and the linear SVM. In the data coding phase, constellations are shaped to decrease possible noise and inter-symbol interference (ISI), which shares the equalization pressure at the receiver side. And we choose three kinds of shaped 8QAM constellations to evaluate their performances in the PON system. On the receiver side, we propose to utilize an SVM for signal recovering after a simple LMS equalization. The signal recovering process is converted to a classification problem of the constellation points and SVM can precisely generate decision boundary though the nonlinear distortion of the constellation is serious. Simulation results indicate that at the bandwidth of 25 GHz and an overall bitrate of 50 Gbit/s, system performance can be significantly improved by the proposed constellation shaping joint SVM scheme. Over 37 dB link loss budget is achieved.

2 Principle

2.1 SVM for Modified 8QAM Constellation

By redesigning the distribution of the transmitted signal constellation, geometrically shaping (GS) can improve the minimum Euclidean distance (ED) between constellation points representing different QAM symbols, thus reducing the effects of noise. In this section, we evaluate three special-shaped 8QAM constellations among the GS-8QAM signals. Fig. 1 shows the redesigned constellations. The most commonly used is Circular (4, 4) which divides 8 constellation points into 4 points in the outer ring and 4 points in the inner ring; in addition, we also discuss the rectangular distribution and triangular distribution.

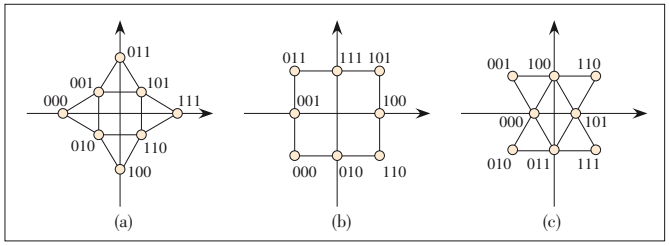

▲ **Figure 1. Constellations of shaped 8 quadrature amplitude modulation (8QAM): (a) Circular (4, 4), (b) rectangular and (c) triangular**

The ratio of the radius of the outer ring to the radius of the inner ring (second outer) is 1.932, 1.414 and 1.414 for Circular (4, 4), Rectangular and Triangular respectively, which refers to the amplitude difference between the symbol points in the three constellations. Apparently, the high amplitude signal induces severer nonlinear impairments to low amplitude signals. Therefore, distortion and compression appear in the constellation points near the outer ring, which destroys the original separable margin and changes the ED between different symbols. This phenomenon is harmful to the ED based signal detection method. We consider the 8QAM constellation set as $\mathcal{M}$ and one received symbol as y_{ij}, and then the ED based signal detection result of y_{ij} can be obtained as:

$$\check{x}_{ij} = \arg\min_{x \in \mathcal{M}} \left| y_{ij} - x \right| . \tag{1}$$

Once the position of y_{ij} deviates a considerable distance from the correct x due to the nonlinear distortion and compression, the detection result of Eq. (1) will go wrong in high probability. However, by searching suitable received symbols in different groups as the support vectors, SVM can effectively find the optimal decision boundaries during groups without the restriction of constellation set $\mathcal{M}$. In the binary classification case, two groups are supposed to be separable if there exists one function which can be expressed as:

$$f(\boldsymbol{x}) = \boldsymbol{w}^T \boldsymbol{x} + b , \tag{2}$$

where $\boldsymbol{w}$ and b denote the weight and bias. Given the training data $\boldsymbol{x}_i$, and $y_i \in \{\pm 1\}$ is the associated label, the function should satisfy that $f(x) > 0$, if $y_i = 1$; $f(x) < 0$, if $y_i = -1$. $f(x) = 0$ acting as a decision boundary toward two regions is called a hyperplane. Those points satisfying $f(x) = \pm 1$ are called support vectors and the distance between $f(x) = \pm 1$ is called margin which equals to $2/\|\boldsymbol{w}\|$. The goal of SVM is to find the optimal support vector such that the margin is maximized. In other words, this is an optimization problem.

$$\begin{aligned} &\underset{\{\boldsymbol{w},b\}}{\text{minimize}} \quad \frac{1}{2} /\!/ \boldsymbol{w} /\!/ ^2 \\ &\text{subject to} \quad y_i\left(\boldsymbol{w}^T \boldsymbol{x}_i + b\right) \geqslant 1, \text{with } i = 1,2,\ldots,n \end{aligned} . \tag{3}$$

For those cases that the data cannot support perfectly linear separating, slack variable $\xi_i > 0$ is introduced:

$$\begin{aligned} &\underset{\{\boldsymbol{w},b\}}{\text{minimize}} \quad \frac{1}{2} /\!/ \boldsymbol{w} /\!/ ^2 + C\sum\nolimits_{i=1}^{n} \xi_i \\ &\text{subject to} \quad y_p\left(\boldsymbol{w}^T \boldsymbol{x}_i + b\right) \geqslant 1 - \xi_i \\ &\quad \xi_i \geqslant 0, i = 1,2,\ldots,n \end{aligned} . \tag{4}$$

If the training data set is assumed to be linearly insepara-

ble, the kernel function can be used to map the origin input vectors into a linearly separable space. In this paper, shaped 8QAM constellation classifications are treated as linear separable problems. Therefore, the detailed derivation for SVM classifiers using kernel function is not discussed here and can be found in Refs. [13 – 14].

Detection of the shaped 8QAM constellation is an eight-class classification problem. However, we can build a binary SVM classifier between each one class and the rest seven classes, so the results of eight binary SVM classifiers can solve the eight-class classification problem[15 – 16]. This problem can be trained in many efficient ways[17 – 18]. After training, the workflow of an SVM classifier is shown in Fig. 2(a). At first, the input feature vector is normalized by a linear kernel function. Then the normalized feature that joints a few support vectors is fed into the sign(•) function for decision. Finally, the decision output vector is decoded to get the final classification result.

In fact, the training process of SVM is to find the optimal support vectors which decide $\boldsymbol{w}$ and the hyperplane. So, when the shaped 8QAM constellation suffers from distortions and compression after the transmission in the PON channel, the position changes of the support vectors will rearrange the hyperplane. Figs. 2(a) and 2(b) show the influence of nonlinearity on the constellation points and the hyperplanes. In Figs. 2(a) and 2(b), the blue ball denotes the constellation points of the outer ring and the red ball denotes the constellation points of the inner ring. Owing to the nonlinear response of the channel, the outer ring will be compressed more severely than the inner ring, which results in the approaching of the blue ball and the red ball. And then from Fig. 2(a) to Fig. 2(b), the support vectors picked from the colored balls will direct the hyperplanes to new positions, while the ED decision method still holds its eight decision areas on the three kinds of shaped 8QAM constellations. Points in the compressed 8-QAM constellation are easy to fall on the wrong ED decision areas due to annoying noise but the SVM can figure out the compression and reflect on the changes of decision boundaries. As a result, the SVM classifier appears more stable and accurate than the ED decision method.

2.2 Adaptive Volterra Filter

Volterra filters are commonly used to model nonlinear responses and compensate for nonlinear effects in IM/DD systems[17]. An n-th order Volterra filter can be expressed as:

$$y(n) = \sum_{n=1}^{N}\left[\sum_{k_1=0}^{M-1}\cdots\sum_{k_n=k_{n-1}}^{M-1} a_n\left(k_1,\ldots,k_n\right)x\left(n-k_1\right)\ldots x\left(n-k_n\right)\right], \tag{5}$$

where M represents the memory length and a_n is the n-th order Volterra kernels.

The coefficients of the second-order Volterra filter can be searched by using the LMS adaptive structure in Ref. [18], and the algorithm is described as

$$\begin{aligned}&\boldsymbol{a}_1(k+1) = \boldsymbol{a}_1(k) + \mu\boldsymbol{e}_k\\&\left[\boldsymbol{a}_2(k+1)\right] = \left[\boldsymbol{a}_1(k)\right] + \mu e_k\boldsymbol{x}\boldsymbol{x}^T\\&\boldsymbol{e}_k = \boldsymbol{d}_k - \boldsymbol{y}_k,\end{aligned} \tag{6}$$

where μ controls the magnitude of the weight adjustment, $\boldsymbol{x}$ is the $M\times1$ input vector, $[\boldsymbol{a}_2]$ is a coefficients matrix containing the second-order kernel factors, and $\boldsymbol{e}_k$ represents the error. In

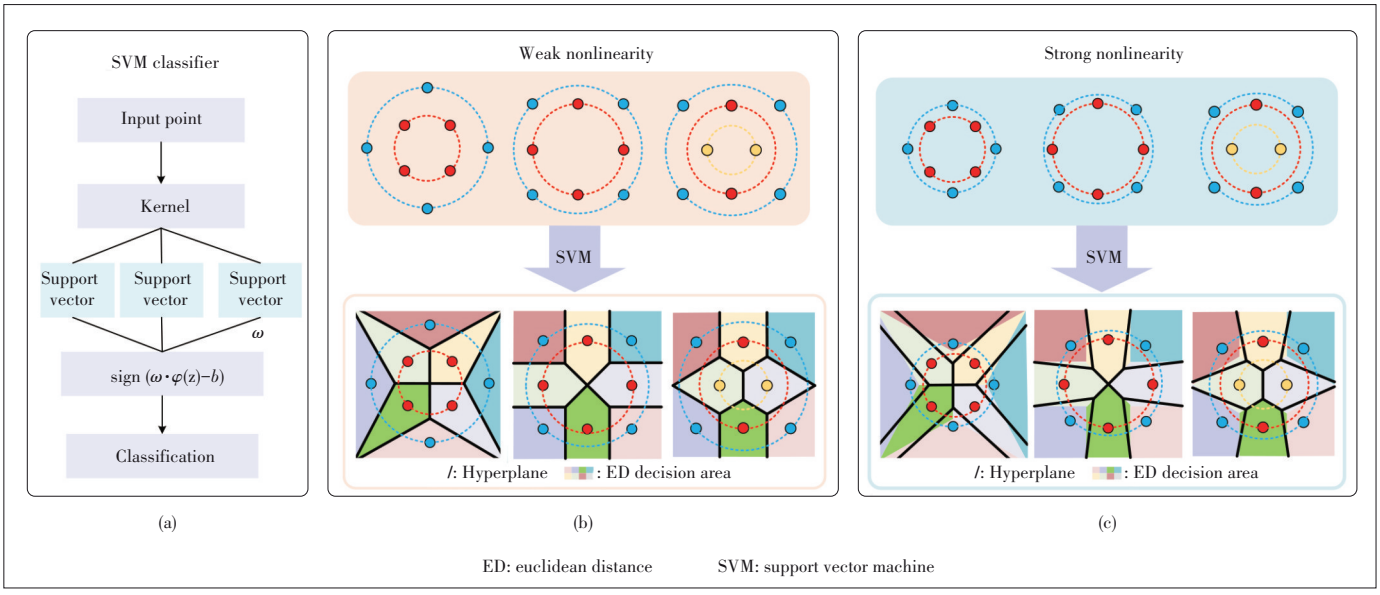

▲ **Figure 2. (a) Flow chart of SVM classifier, (b) nonlinear distortions of the three constellations and (c) their influences on hyperplanes of the SVM classifier**

this work, the second-order LMS-based Volterra filter (LMS-VOT) is implemented to equalize distortions in the received signal and compare the performance with the SVM based scheme.

3 Simulation Setup

The PON system simulation is carried out in the VPItransmissionMaker™. In the simulation setup shown in Fig. 3(a), bandwidth limitations, dispersion, and nonlinearity of the fiber link are considered. At the transmitter (Tx) side, to simulate a bandwidth-constrained system, the electrical signal generated from Tx DSP is passed through a 25 GHz low-pass fourth-order Bessel filter before being input into the electro-absorption modulator (EAM). On the other branch, the laser generates a 228.33 THz continuous wave (CW) and also inputs it into the EAM. The transmission characteristic of EAM is determined by the manual defined nonlinear transfer curve in Fig. 3(b). From the curve we can find as the input voltage increases, the modulated output of EAM suffers from saturation influence and severe nonlinear distortions occur. Then the modulated optical signal is fed into a bandpass optical filter to generate a single sideband (SSB) signal. This operation can reduce the power decay caused by dispersion. For flexible control of the transmit power, the output signal from the filter is passed through an optical amplifier. And then the signal is transmitted to the optical distribution network (ODN) through a 20 km long standard single mode fiber (SSMF) with an attenuation of 0.32E-3 dB/m. The output signal of the fiber is connected to two 1×8 splitters to simulate the multi-user network. And the followed attenuator (ATT) controls the link loss, together with the budget for other losses in the link, resulting in a total attenuation of 32 dB from the Tx to the receiver side (Rx). The current signal from the avalanche photodiode (APD) is converted into the voltage signal by a transimpedance amplifier (TIA). Afterward, the voltage signal is analyzed by off-line Rx DSP. Except for the above-mentioned parameters, the rest simulation parameters are summarized in Table 1.

In the Tx DSP, constellation shaped 8QAM symbols are generated and then oversampled to 4 samples per symbol. The orthogonal square-root-raised cosine (SRRC) shaping filter

▼**Table 1. Simulation parameters**

Parameter	Value	Parameter	Value
Data rate	50 Gbit/s	Dispersion slope of SSMF	0.086E3 s/m^3
Signal format	shaped 8QAM CAP	Nonlinear index of SSMF	2.6E-20 m^2/W
Sample rate	200/3 GHz	Responsivity of APD	0.8 A/W
Filter type	Fourth-order Bessel	Dark current multiplied of APD	300E-9 A
Tx signal wavelength	1 310 nm	Avalanche multiplication of APD	8
Length of SSMF	20 km	Ionization coefficient of APD	0.4
Attenuation of SSMF	0.32E-3 dB/m	Transimpedance of TIA	1 000 Ω
Dispersion of SSMF	0.35E-5 s/m^2	Input equivalent noise of TIA	1.1E-6 A

APD: avalanche photodiode
CAP: carrierless amplitude and phase
SSMF: standard single mode fiber
TIA: transimpedance amplifier
Tx: transmitter

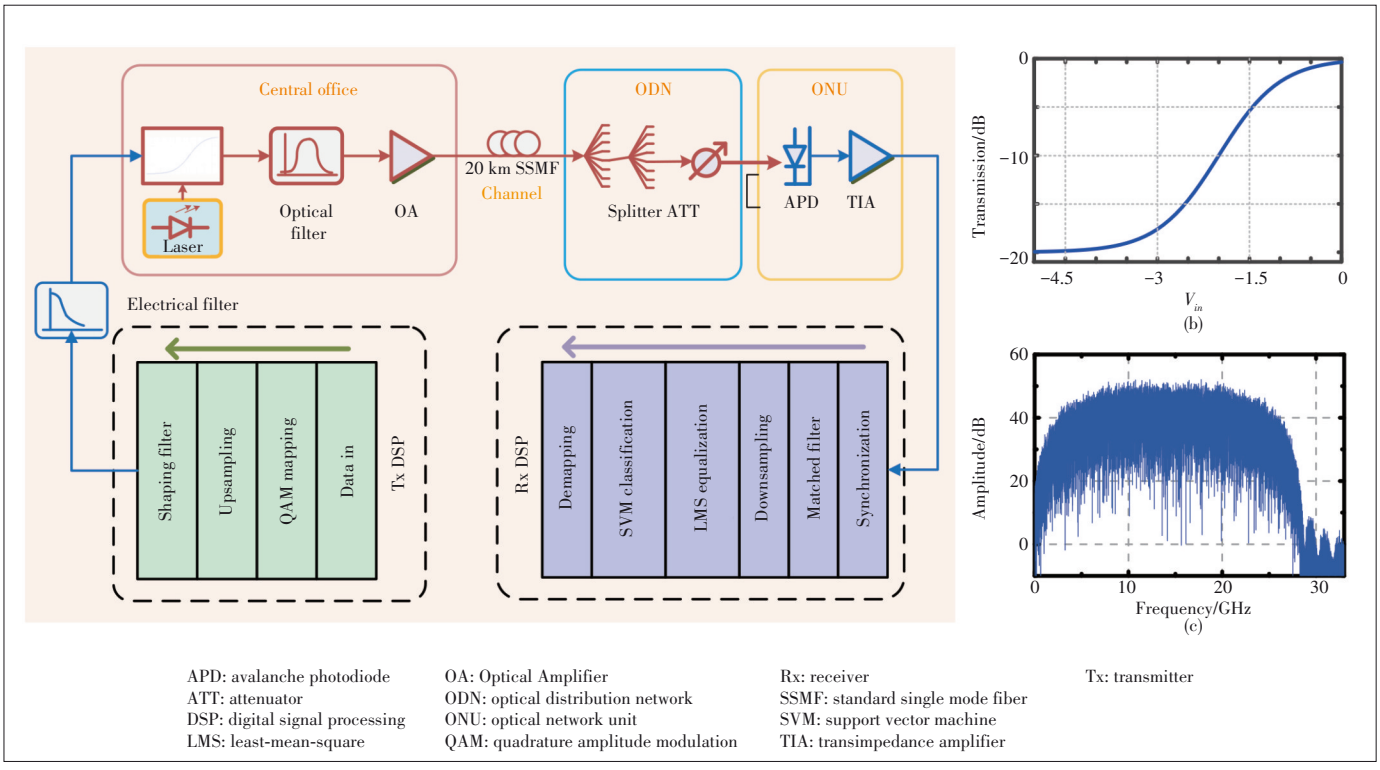

APD: avalanche photodiode
ATT: attenuator
DSP: digital signal processing
LMS: least-mean-square
OA: Optical Amplifier
ODN: optical distribution network
ONU: optical network unit
QAM: quadrature amplitude modulation
Rx: receiver
SSMF: standard single mode fiber
SVM: support vector machine
TIA: transimpedance amplifier
Tx: transmitter

▲**Figure 3. (a) Simulation setup of constellation shaped 8QAM PON system, (b) spectrum of the transmitted signal and (c) electro-absorption modulator (EAM) transmission characteristic**

pairs containing I/Q channels with a variable roll-off are applied to get the carrierless amplitude and phase (CAP) modulated signal. Fig. 3(c) shows the electric spectrum of the modulated Tx signal. The Rx DSP consists of a synchronization module, matched SRRC filter pairs to extract the in-band signal, a down-sampler that generates one symbol for every four samples, a simple LMS equalizer, a multi-class SVM classifier, and a QAM decoder to convert the SVM output symbols into bitstreams for calculating the bit error ratio (BER) of the recovered signal.

Before launching the performance evaluation, the optimal operating state of the Tx signal is investigated by measuring the BER of Circular (4, 4) based 8QAM PON system under different roll-off of the shaping filter, bias of the laser, and linewidth of the laser. From results shown in Figs. 4(a) and 4(d), as the roll-off and bias increase, we can see the BER reaches the minimum and then rises. The maximal BER difference between LMS and LMS+SVM is 5.4E-3 in Fig. 4(d). Similar results also can be observed in Fig. 4(b), where the trend suggests that the PON channel generates different degrees of fiber dispersions according to different wavelengths. To minimize the dispersion effect, we fix the wavelength of the laser at 1 310 nm. Although the linewidth of the laser needs to be as lower as possible, practical low-cost applications cannot promise the narrowest linewidth. So taking the real condition and the above results into account, we set the appropriate roll-off, linewidth and bias as 0.7, 1E6 and −1.4. With these fixed parameters we conduct the rest evaluation work.

4 Results and Analysis

To present the nonlinearity distortion in the simulated system, we investigate the performance of BER versus amplitude of the Tx signal, as shown in Fig. 5. We fix the bias of the laser and then adjust the amplitude of the laser driver. As the amplitude increases, a turning point appears at the bottom of the performance curves of all the three shaped 8QAM constellations, showing that larger amplitude not only brings higher SNR but also induces more severe nonlinearity. From the three constellations shown in Fig. 5, corresponding to circled-out optimal points, we can observe nonlinear influences of the points group at the outer ring is diffuse and their envelopes are elliptical but not circular. Fig. 6 shows the difference between strong nonlinearity and weak nonlinearity in three kinds of constellations. The warm color area is the place where plenty of points are converged while the cool color means the points have diverged. And by comparing the color of the outer ring with the inner ring, it is clear that those constellations under strong nonlinearity suffer more distortions. When the non-

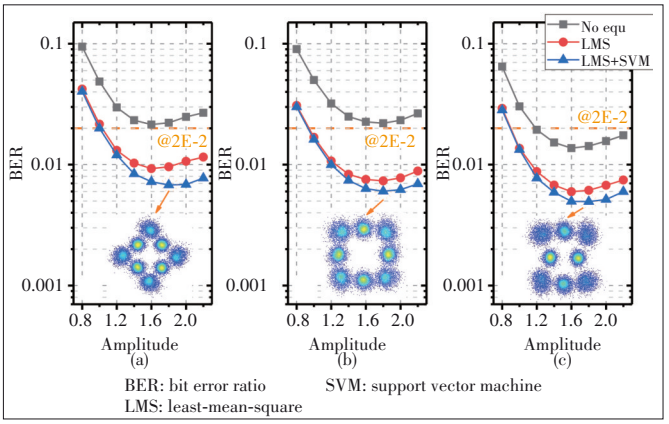

▲Figure 5. BER performance versus amplitude of the Tx signal (a) Circular (4, 4), (b) Rectangular and (c) Triangular

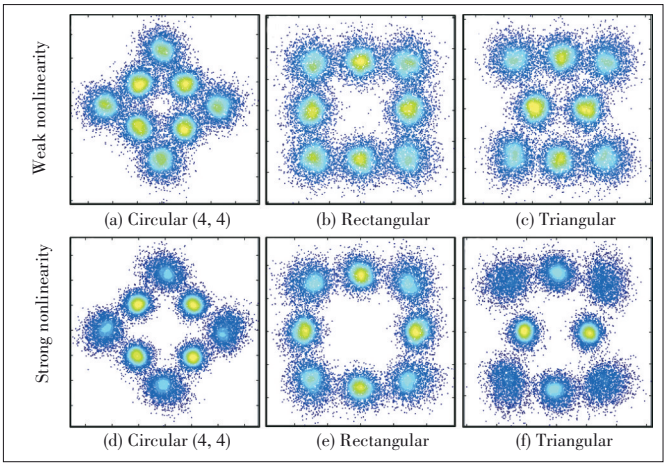

▲Figure 6. Distortions under different levels of nonlinearity

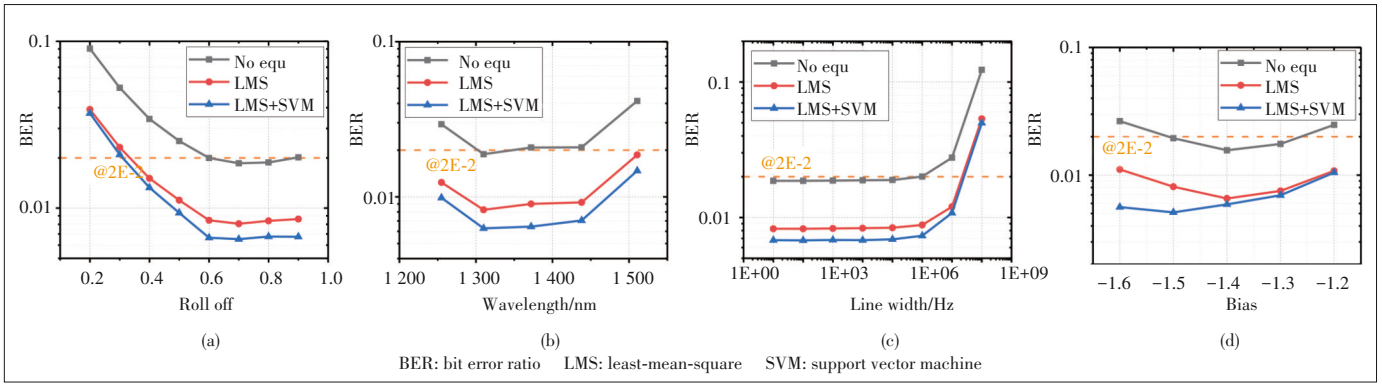

▲Figure 4. BER of Circular (4, 4) versus (a) roll off of shaping filter, (b) wavelength of LD, (c) line width of LD and (d) bias of laser

linear impairments overcome the SNR gains, the system BER stops decreasing. By training the LMS equalizer with 2 000 samples of the waveform sequence, the equalized BER performance can be well below the 0.02 FEC threshold. However, as is shown in Fig. 7, when the constellation distortions occur, because the ED decision method will not change the decision boundaries which has been already decided as the GS coding completes, the performance can be further improved by using the SVM classifiers to redistribute the hyperplanes between distorted groups of constellation points. Moreover, the boundary changes between the SVM classifier and ED decision method are more obvious in the Circular (4, 4) constellation than the Rectangular and Triangular constellations. This phenomenon can be explained by the difference in the ratios mentioned in Section 2, the larger radius ratio of Circular (4, 4) results in a larger amplitude difference between the symbols on the outer ring and the inner ring. Taking the amplitude as the input of the function in Fig. 3(b), the nonlinear output differs as the input changes. Thus, if the amplitude difference is large, the nonlinear response is more apparent. As a result, Circular (4, 4) suffers more distortions and the hyperplanes appear more different from the ED decision boundaries than the other two constellations.

The results above mainly display the nonlinear influence on three kinds of constellations. The following part will discuss the performance of three equalization schemes on the BER, power budget, and complexity. First, we research the performance of BER versus bandwidth. In Fig. 8, as the bandwidth limitation increases, three shaped 8QAM signals all demonstrate better performance. The BER improvement after using SVM is remarkable in Circular (4, 4), indicating that it benefits more from the SVM classifier because of its stronger nonlinear distortions. The rectangular constellation has the worst performance in that the BER of the recovered signal is still greater than the 0.02 FEC threshold, when no equalization is applied. And the performance ranking of the three equalizers is LMS-SVM the first, LMS-VOT the second, and LMS the last. When the bandwidth reaches 25 GHz, the performance of three kinds of constellations is still unsatisfactory for they do not reach the hard-decision FEC (HD-FEC) threshold (3.8E-3). Therefore, we continue to study the BER performance versus the receiver sensitivity. Fig. 9 shows that the BER improves significantly as the received power increases. As the received power reaches −21 dBm, all kinds of constellations satisfy the HD-FEC threshold. The Triangular appears more suitable for transmitting in the PON channel for it meets the 3.8E-3 threshold even without the assistance of the SVM classifier. But the SVM classifier helps Circular (4, 4) reach the lowest BER among all results at present, which suggests the superiority of the SVM classifier in the nonlinear circumstance. From Fig. 9 we can also get the receiver sensitivity as approximately −21.5 dBm because the BERs approach 3.8E-3 with all three kinds of constellations at −21.5 dBm Rx power. Therefore, the

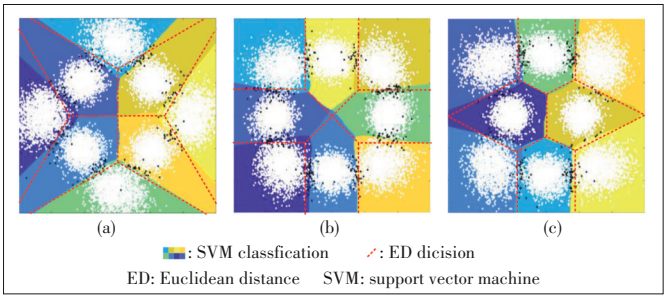

▲ **Figure 7. The classification results of SVM and ED decision: (a) Circular (4, 4), (b) Rectangular and (c) Triangular**

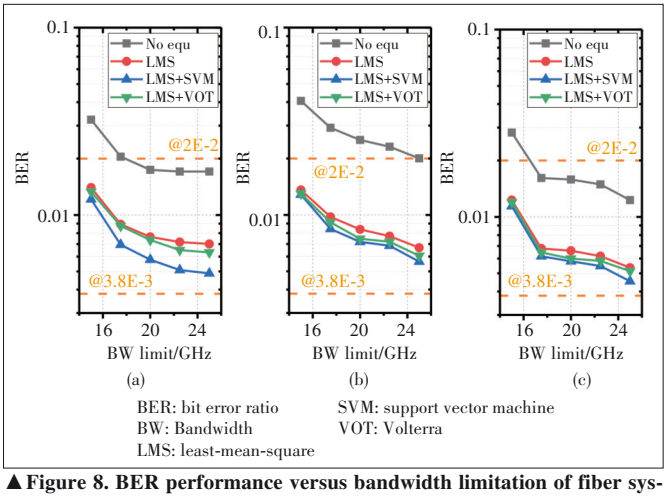

▲ **Figure 8. BER performance versus bandwidth limitation of fiber system: (a) Circular (4, 4), (b) Rectangular and (c) Triangular**

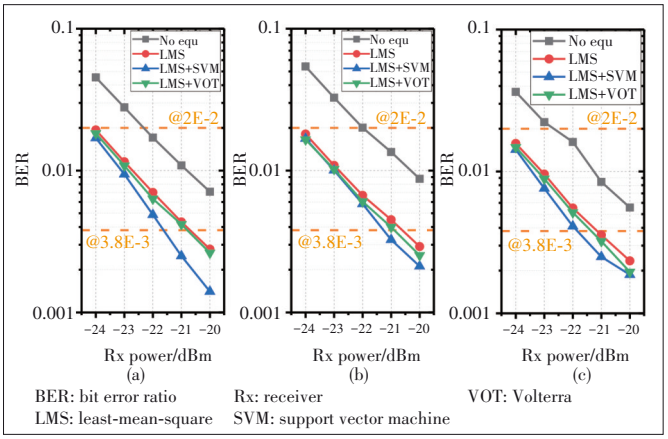

▲ **Figure 9. BER performance versus received power: (a) Circular (4, 4), (b) Rectangular and (c) Triangular**

received power is fixed to −21.5 dBm to analyze the power budget of the PON system in Fig. 10. The curve suggests that Circular (4, 4) achieves the lowest transmitting power requirements of 3.98 dBm. The BER performance gap between LMS-SVM and the other three methods is very significant in Circular (4, 4), which is explained by the larger radius ratio and thus more severe distortions. For Rectangular and Triangular, the transmitting power should increase to 10.79 dBm and 8.75 dBm separately so that the BERs can meet the HD-FEC threshold. It is meaningful that the Circular (4, 4) joint LMS-

SVM solution has saved at least 4.77 dB of input power compared with the solutions transmitting the other two constellations. Due to fiber nonlinearity impairments, as the fiber input power increases, the BER performance of all of the three solutions is getting worse. The same maximum power budget of 37.52 dB is achieved after 20 km SSMF in all three solutions. In Figs. 9 and 10 we can also find that the Triangular constellation performs the best if all three constellations are just equalized by LMS, which may draw interest if the extremely low complexity in PON system is required.

Furthermore, we make a comprehensive complexity comparison of the three equalization methods and the computational costs are listed in Table 2 in terms of the multiplications and additions. The computational complexity differs at the training stage and the prediction stage because the training processes contain extra weights updating procedure. The LMS and the LMS-VOT equalizers process the waveform of the Rx signal while the SVM classifier deals with the signal constellations. So, the complexity of SVM depends on different parameters with the LMS and LMS-VOT algorithms. In Table 2, T_1 is the length of the training waveform sequence for LMS and LMS-VOT, T_2 is the number of the training symbols for SVM, N_s is the number of support vectors, d is the dimension of classification results, and M_1 and M_2 refer to the tap numbers of the first order and the second order adaptive filter. In this simulation, T_1 = 2 000, T_2 = 800, d = 8, M_1 = M_2 = 15, and N_s is a variable that varies as the hyperplanes adjust. Since in 8QAM constellations only a few points satisfy $f(x) = \pm 1$ in Eq. (2) and most of the constellation points locate far from the hyperplane, the typical value of N_s is much smaller than T_2, approximately 10% of T_2. Taking a specific value N_s = 80 into account, the computational complexity of SVM is O (512 640) while the LMS-VOT algorithm contains 754 000 additions and 994 000 multiplications at the training stage. It needs to be addressed that the LMS-VOT just uses the first and the second order Volterra kernels. Further increasing the order of kernels will bring unacceptable computational costs for the PON system. After training every time in the prediction procedure, the complexity of the proposed SVM is O (640), the same level as the LMS-VOT algorithm that makes 136 additions and 255 multiplications. The above analysis suggests that by limiting the number of the training symbols, the computational cost of the proposed linear SVM, together with the LMS equalizer, is well controlled at both stages compared with the classic LMS-VOT adaptive filter. Above all, the proposed LMS-SVM scheme promises better BER performance at a well-controlled computational complexity for the PON system.

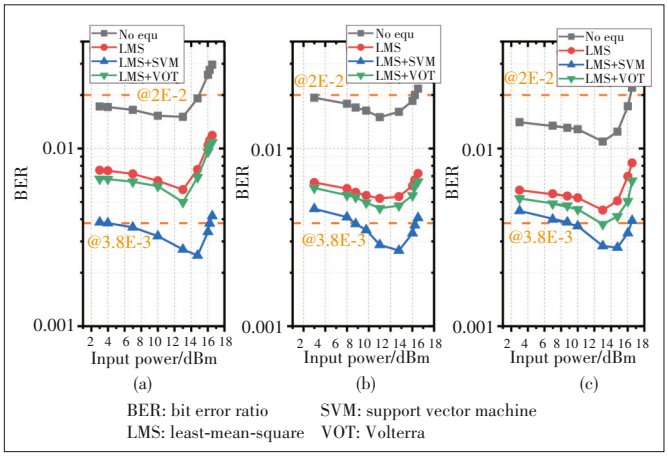

▲ **Figure 10. BER performance versus fiber input power: (a) Circular (4, 4), (b) Rectangular and (c) Triangular**

5 Conclusions

Nonlinearity impairments and distortions have been bothering the bandwidth constrained PON system for a long time and limit the development of capacity in the PON system. To mitigate impairments accumulated in optical components and PON channels, we propose a low computational complexity and efficient constellation shaped 8QAM joint SVM scheme. On the transmitter side, three kinds of shaped 8QAM constellations are generated to resist the influence of noise and distortions. On the receiver side, simple multi-class linear SVM classifiers are utilized to replace complex equalization methods. The hyperplane generation process of SVM and the nonlinear influence on hyperplane are discussed to explain why SVM is superior to the Euclidean distance decision method. Simulation results show that with the bandwidth of 25 GHz, overall bitrate of 50 Gbit/s, and under hard-decision FEC threshold, transmission can be realized by employing Circular (4, 4) shaped 8QAM joint SVM classifier at the maximum pow-

▼**Table 2. Computational complexity**

Methods	Training		Prediction	
	Additions	Multiplications	Additions	Multiplications
LMS	$(M_1 + M_1 + 1)T_1$	$(M_1 + M_1 + 1)T_1$	M_1	M_1
LMS-VOT	$(2M_1 + \frac{M_2(M_2+1)}{2} + M_2^2 + 2)T_1$	$(2M_1 + M_2(M_2+1) + M_2^2 + 2)T_1$	$M_1 + \frac{M_2(M_2+1)}{2} + 1$	$M_1 + M_2(M_2+1)$
SVM [19]	$O(N_s^2 + N_s dT_2)$		$O(N_s d)$	

M_1 is the tap number of the linear part, M_2 is the tap number of the nonlinear part, T_1 is the length of the training sequence, T_2 is the number of the training symbols, N_s is the number of support vectors and d is the dimension of classification.
LMS: least-mean-square SVM: support vector machine VOT: Volterra

er budget of 37.5 dB. And at least 4.77 dB input power difference occurs between Circular (4, 4) and the other two constellations by using SVM, which indicates the Circular (4, 4) shaped 8QAM joint SVM classifier is more suitable to be transmitted in the PON system with lower input power and less nonlinear distortions.

References

[1] IEEE. Physical layer specifications and management parameters for 25 Gbit/s and 50 Gbit/s passive optical networks: IEEE 802.3ca Task Force [S]. 2018
[2] HOUTSMA V, VEEN DVAN. Optical strategies for economical next generation 50 and 100G PON [C]//Optical Fiber Communication Conference. OFC, 2019. DOI:10.1364/ofc.2019.m2b.1
[3] JI H L, YI L L, LI Z X, et al. Field demonstration of a real-time 100-Gbit/s PON based on 10G-class optical devices [J]. Journal of lightwave technology, 2017, 35(10): 1914 – 1921. DOI: 10.1109/JLT.2016.2633482
[4] HOUTSMA V, VEEN DVAN. Demonstration of symmetrical 25 Gbit/s TDM-PON with 31.5 dB optical power budget using only 10 Gbit/s optical components [C]//2015 European Conference on Optical Communication. IEEE, 2015: 1 – 3. DOI:10.1109/ECOC.2015.7341691
[5] WEI J L, EISELT N, GRIESSER H, et al. Demonstration of the first real-time end-to-end 40-Gbit/s PAM-4 for next-generation access applications using 10-Gbit/s transmitter [J]. Journal of lightwave technology, 2016, 34(7): 1628 – 1635. DOI:10.1109/JLT.2016.2518748
[6] IEEE. Ethernet amendment 10: media access control parameters, physical layers, and management parameters for 200 Gbit/s and 400 Gbit/s 802.3bs-2017: IEEE 802.3bs-2017 [S]. 2017
[7] ZHANG J, YU J J, CHIEN H, et al. Demonstration of 100 Gbit/s/λ PAM-4 TDM-PON supporting 29 dB power budget with 50 km reach using 10 G class O-band DML transmitters [C]//Optical Fiber Communication Conference Post-deadline Papers. OSA, 2019. DOI:10.1364/ofc.2019.th4c.3
[8] ZHANG J W, YU J J, LI F, et al. 11 × 5 × 93 Gbit/s WDM-CAP-PON based on optical single-side band multi-level multi-band carrierless amplitude and phase modulation with direct detection [J]. Optics express, 2013, 21(16): 18842. DOI: 10.1364/oe.21.018842
[9] WEI J L, INGHAM J D, CUNNINGHAM D G, et al. Performance and power dissipation comparisons between 28 Gbit/s NRZ, PAM, CAP and optical OFDM systems for data communication applications [J]. Journal of lightwave technology, 2012, 30(20): 3273 – 3280. DOI:10.1109/JLT.2012.2213797
[10] YIN S, HOUTSMA V, VEEN DVAN, et al. Optical amplified 40-Gbit/s symmetrical TDM-PON using 10-Gbit/s optics and DSP [J]. Journal of lightwave technology, 2017, 35(4): 1067 – 1074. DOI: 10.1109/JLT.2016.2614767
[11] WANG C, DU J B, CHEN G Y, et al. QAM classification methods by SVM machine learning for improved optical interconnection [J]. Optics communications, 2019, 444: 1 – 8. DOI: 10.1016/j.optcom.2019.03.058
[12] NIU W Q, HA Y, CHI N. Support vector machine based machine learning method for GS 8QAM constellation classification in seamless integrated fiber and visible light communication system [J]. Science China information sciences, 2020, 63(10): 202306. DOI: 10.1007/s11432-019-2850-3
[13] SAIN S R. The nature of statistical learning theory [J]. Technometrics, 1996, 38(4): 409. DOI: 10.1080/00401706.1996.10484565
[14] HSU C W, LIN C J. A comparison of methods for multiclass support vector machines [J]. IEEE transactions on neural networks, 2002, 13(2): 415 – 425. DOI: 10.1109/72.991427
[15] JOACHIMS T. Training linear SVMs in linear time [C]//The 12th ACM SIGKDD International Conference on Knowledge Discovery and Data Mining. ACM, 2006: 217 – 226. DOI: 10.1145/1150402.1150429
[16] KEERTHI S S, DECOSTE D. A modified finite Newton method for fast solution of large scale linear SVMs [J]. Journal of machine learning research, 2005, 6(12):341–361
[17] CHEN K Z, CHEN L W, LIN C Y, et al. 224-Gbit/s transmission for next-generation WDM long-reach PON using CAP modulation [C]//2016 Optical Fiber Communications Conference and Exhibition (OFC). IEEE, 2016: 1 – 3
[18] STOJANOVIC N, KARINOU F, QIANG Z, et al. Volterra and Wiener equalizers for short-reach 100 G PAM-4 applications [J]. Journal of lightwave technology, 2017, 35(21): 4583 – 4594. DOI: 10.1109/JLT.2017.2752363
[19] BURGES C J C. A tutorial on support vector machines for pattern recognition [J]. Data mining and knowledge discovery, 1998, 2(2): 121 – 167. DOI: 10.1023/A: 1009715923555

Biographies

LI Zhongya is with the Department of Communication Science and Engineering, School of Information Science and Technology, Fudan University, China.

CHEN Rui is with the Department of Communication Science and Engineering, School of Information Science and Technology, Fudan University, China.

HUANG Xingang is a senior expert of technical pre-research of ZTE Corporation. He received the M.S. degree in physics from Xi'an Jiaotong University, China in 2008. He is engaged in the research of optical access technology, especially in WDM-PON, TWDM-PON, NG-EPON, 50 G PON.

ZHANG Junwen is with the Department of Communication Science and Engineering, School of Information Science and Technology, Fudan University, China.

NIU Wenqing is with the Department of Communication Science and Engineering, School of Information Science and Technology, Fudan University, China.

LU Qiuyi is with the Department of Communication Science and Engineering, School of Information Science and Technology, Fudan University, China.

CHI Nan (nanchi@fudan.edu.cn) is with the Department of Communication Science and Engineering, School of Information Science and Technology, Fudan University, China.